LA-UR- 85-752

CONF-850310--44

LA-UR--85-752

DE85 009591

TITLE A COMPARISON STUDY OF TOROIDAL-FIELD DIVERTORS FOR A COMPACT REVERSED-FIELD PINCH REACTOR

AUTHOR(S) C. G. Bathke, R. A. Krakowski, and R. L. Miller
Los Alamos National Laboratory
Los Alamos, New Mexico 87545

SUBMITTED TO 6th ANS Topical Meeting on the Technology of Fusion Energy, San Francisco, CA
March 3-7, 1985

DISCLAIMER

Los Alamos Los Alamos National Laboratory
Los Alamos, New Mexico 87545

A COMPARISON STUDY OF TOROIDAL-FIELD DIVERTORS FOR A COMPACT REVERSED-FIELD PINCH REACTOR*

C. G. Bathke, R. A. Krakowski, and R. L. Miller
Los Alamos National Laboratory, Los Alamos, New Mexico 87544
(505)667-7214

ABSTRACT

Two divertor configurations for the Compact Reversed-Field Pinch Reactor (CRFPR) based on diverting the minority (toroidal) field have been reported. A critical factor in evaluating the performance of both poloidally symmetric and bundle divertor configurations is the accurate determination of the divertor connection length and the monitoring of magnetic islands introduced by the divertors, the latter being a three-dimensional effect. To this end the poloidal-field, toroidal-field, and divertor coils and the plasma currents are simulated in three dimensions for field-line tracings in both the divertor channel and the plasma-edge regions. The results of this analysis indicate a clear preference for the poloidally symmetric toroidal-field divertor. Design modifications to the limiter-based CRFPR design that accommodate this divertor are presented.

I. INTRODUCTION

Magnetic divertors are an alternative to the pumped-limiter impurity control scheme invoked by the Compact Reversed-Field Pinch Reactor (CRFPR) design.[1,2] Limiters have the well-known uncertainties related to erosion and the resultant plasma contamination. Impurity-control experiments in tokamaks[3-5] indicate improved energy and particle confinement for plasmas operated with a magnetic divertor which thermally insulates the the plasma and inhibits the return of particles to the plasma from the neutralizer plate.

Magnetic divertors can be classified according to: a) the field component being nulled, or b) the geometry of the field null. With respect to the latter, the field null can encircle the plasma either completely or partially as in the symmetric or bundle divertors, respectively, considered herein.

*Work performed under the auspices of the US Department of Energy, Office of Fusion Energy

Generally, the minority field is the preferred component to null (i.e., the poloidal field for a tokamak and the toroidal field for an RFP). Nulling the minority field minimizes the magnetic-field perturbation at the plasma edge, minimizing adverse affects on the pressure and the particle or energy confinement times.[5] The efficiency with which particles enter the divertor is increased by minimizing the magnetic mirror depth at the divertor throat, which also is accomplished by nulling the minority field. Lastly, divertor-coil currents scale linearly with the magnitude of the nulled field component, the energy stored in, forces on, and power consumed by the divertor coils are all minimized by nulling the minority field component. Nulling the toroidal field in an RFP, however, does raise concerns about the stability of an RFP plasma with a non-monotonic surface-averaged $q(\equiv B_\phi r_p/B_\theta R)$ profile, relatively large toroidal gaps in the first wall, and a general breaking of the preferred toroidal symmetry.

A preliminary study[6] of the range of the divertor options determined that two kinds of divertors are best suited to the RFP magnetic geometry, a toroidal-field, poloidally symmetric divertor (SD) and a toroidal-field, bundle divertor (BD). The Ref. 6 study was based on a two-dimensional vacuum-field model and could not select a preferred approach. The focus of the present study is a three-dimensional magnetics analysis of the SD and BD designs suggested in Ref. 6. The three-dimensional magnetics provides a more accurate calculation of the divertor connection length (i.e., the distance along a field line between divertor collector plates) as well as a measure of flux surface integrity based on magnetic-island widths arising from a periodic toroidal-field ripple and the thickening of flux surfaces caused by non-axisymmetric toroidal-field ripple.

The design philosophy and reactor configuration are described in Sec. II.A., and the model used for simulating the plasma is given in Sec. II.B. The results of three-dimensional magnetics simulations for the reference design without divertors, with BDs,

and with SDs are presented in Sec. III. In addition, design parameters are given for the preferred divertor design: the toroidal-field, poloidally symmetric divertor. Section IV. summarizes the critical elements of the SD design.

II. MODEL

A. Design Constraints

The limiter-based CRFPR design to which divertors will be added is taken from Ref. 1, amplified in Ref. 7, and summarized in Table I. The Ref. 7 design is based on an additional 0.10-m-thickness added to the blanket ($\Delta b = 0.775$), although the Ref. 1 design is retained for this divertor study in anticipation of improved blanket performance (i.e., low heat loads, no limiter, eased tritium breeding) for the divertor case. A minimum shield thickness of 0.1-m is required between the plasma and the divertor coils, and an $x_\ell = 0.04$-m-thick scrapeoff layer is positioned between the separatrix and first wall. The current density in the divertor coils is constrained to be below 50 MA/m^2, following the MARS choke coil design.[8] Four SDs or eight BDs were deemed necessary[6] to maintain the heat flux to the plasma-chamber and the divertor-channel walls below 6 MW/m^2. Outboard maintenance of either divertor imposes an additional constraint on both divertor size and poloidal field coil (PFC) and TFC location.

TABLE I
KEY CRFPR DESIGN PARAMETERS[1]

Parameter	Value
Fusion power, P_F(MW)	2732
Thermal power, P_{TH}(MW)	3365
Net electric power, P_E(MWe)	1000
Neutron wall loading, I_w(MW/m^2)	19.5
Reversal surface radius, r_v	0.64
Plasma minor radius, r_p(m)	0.71
First-wall radius, r_w(m)	0.75
Plasma major radius, R_T(m)	3.80
Blanket/shield thickness, Δb(m)	0.675
Number of TFCs, N_{TF}	24
Toroidal field, $B_\phi(r_p)$(T)	0.403
Poloidal field , $B_\theta(r_p)$(T)	5.18
Toroidal plasma current, I_ϕ(MA)	18.4
Pinch parameter, $\Theta = B_\theta(r_p)/\langle B_\phi\rangle$	1.55
Reversal parameter, $F = B_\phi(r_p)/\langle B_\phi\rangle$	-0.12
Poloidal beta, β_θ	0.23
Plasma transport power, P_{TR}(MW)	571.8
Plasma density, n(10^{20}/m^3)	6.55
Plasma temperature, T(keV)	20.
Confinement time, τ_{p1}(s)	0.59
Edge safety factor, $q = \lvert r_p F/\mathcal{R}_T\rvert$	0.015
COE (mills/kWeh)	46.2

B. Plasma Simulation

The first stage of the divertor design proceeds on the basis of a two-dimensional layout. The separatrix is located by field-line tracings that are confined to the equatorial plane and sample a region near the plasma surface. At this stage of analysis, only the divertor coils and the TFC set are simulated with the otherwise three-dimensional vacuum-magnetics code, TORSIDO.[9] The coil locations, currents, and current densities are key design variables. Coils are positioned to minimize and symmetrize the field ripple produced by the divertor; the coil currents were adjusted to locate the separatrix at the plasma surface (Table I); and the coil current densities are determined by requiring no field line to intersect the coils.

B.1. MHD Model. Determination of the divertor connection length and flux-surface integrity (i.e., magnetic islands and flux-surface broadening) can be accomplished only with a three-dimensional model that simulates both the PFCs and the plasma in addition to the TFC and the divertor coil currents. The plasma simulation is based on a one-dimensional MHD model of RFP magnetic field and current density profiles,[1] which solves the following set of simultaneous equations:

$$\vec{j}\times\vec{B} = \vec{\nabla}p \tag{1}$$

$$\vec{\nabla}\times\vec{B} = \mu_0\vec{j} \tag{2}$$

$$\mu = \mu_0\frac{(\vec{j}\cdot\vec{B})}{B^2}, \tag{3}$$

where $\mu_0 = 4\pi(10)^{-7}$ h/m. The pressure profile is described by $p(r) = J_0^2(2\Theta r/r_p)$, where $\Theta = B_\theta(r_w)/\langle B_\phi\rangle$ is the pinch parameter. The normalization of the pressure profile is adjusted iteratively in order to obtain a specific poloidal beta, $\beta_\Theta = 2\mu_0\langle p\rangle/B_\theta^2(r_p)$. In Ref. 1, $\mu(r) = 1$ for $0 \le r \le r_b$ and then ramps linearly to zero for $r_b \le r \le r_p$ (i.e., the Modified Bessel-function Model). This break point, r_b, is determined experimentally[10] to be at $r_b = 0.807r_p$ for $\theta = 1.55$ and causes discontinuities in the radial derivatives of the current density and magnetic field profiles. These discontinuities can result in large errors for a numerical integration or spline of the profiles. This problem is circumvented in the present calculations by using the following continuous function for the μ profile. $\mu(r) = 1$ for $0 \le r \le r_b'$ and then decays to zero according to the first quarter period of a cosine function for $r_b' \le r \le r_p$. The break point for this μ profile is determined by equating areas under the two μ profiles and occurs at $r_b' = 0.73\cdot r_p$. The magnetic field profiles calculated from the one-dimensional MHD model are shown in Fig. 1, which also compares the procedure used in Ref. 10.

B.2. Magnetics. The plasma-current-density and magnetic-field profiles obtained from Eqs. (1)-(3) are used by the three-dimensional magnetics model. The poloidal field is simulated by a current-carrying hoop conductor positioned in the equatorial plane at R = 3.806 m. The 6-mm displacement outward from

the plasma center line corresponds to the Shafranov shift as applied to an RFP[11]. The toroidal current in the hoop is taken to be 18.4 MA for $r > r_p$ and varies as follows for $r < r_p$:

$$I(r) = r^{-2}\int_0^r j_\phi^{MHD}(r')r'dr' , \qquad (4)$$

where $j_\phi^{MHD}(r)$ is described by a cubic spline fit to the toroidal current-density profile. The toroidal field from the plasma is taken to be zero for $r > r_p$, and for $r < r_p$ is determined from

$$B_\phi(r) = B_\phi^{VAC}(r)\left[1 - \frac{B_\phi^{MHD}(r)}{B_\phi^{MHD}(r_p)}\right] , \qquad (5)$$

where $B_\phi^{VAC}(r)$ is the toroidal vacuum field and $B_\phi^{MHD}(r)$ is the toroidal-field profile previously calculated. The effects of toroidal ripple on $j_\phi^{MHD}(r)$ and $B_\phi^{MHD}(r)$ in Eqs. (4) and (5) are simulated by scaling the minor radius according to the fluctuations observed in two-dimensional field-line tracings at the reversal surface minor radius, r_v. These plasma poloidal and toroidal fields are added to the vacuum fields calculated by TORSIDO to complete the combined simulation of plasma and coils.

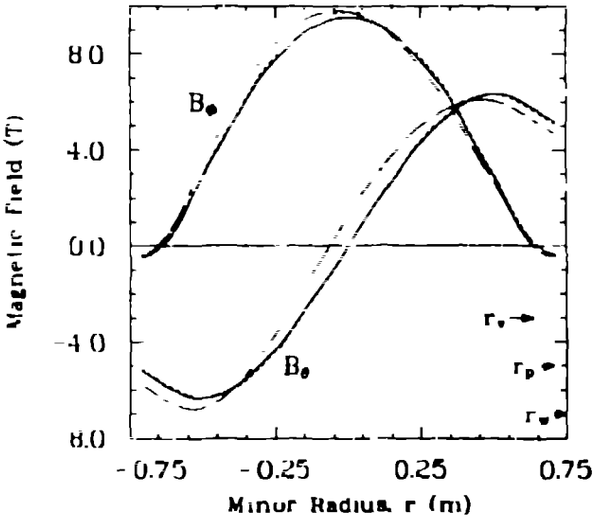

Fig. 1. Magnetic-field profiles from the MHD model using the cosine μ profile (solid lines) and the linear μ profile (dotted lines). Profiles for a vertical cut at R = 3.8 m (dashed lines) and for a horizontal cut at z = 0 m (dashed-dotted lines) are also shown.

III. RESULTS

A. Magnetics of Basic Configuration

The three-dimensional simulation of the plasma, the PFCs, and the TFCs of the basic configuration is shown in Fig. 2. Magnetic islands arising from the toroidal-field ripple with ~ 0.16-m widths were expected based on an infinite-cylinder model[12] using the toroidal-field ripple on the outboard side in the equatorial plane.[1] The field-line tracings revealed, instead, flux "surfaces" with radial widths or volumes. The asymmetry in the toroidal-field ripple, as depicted schematicly in Fig. 3, causes this asymmetry. The toroidally symmetric poloidal flux surfaces connect a set of inboard toroidal-field lines to a set of outboard toroidal-field lines at some toroidal angle, which is taken as a coil plane in Fig. 3. When field lines progress toroidally to a midplane, the poloidal flux surfaces map the set of inboard field lines into a different set of outboard field lines and vice versa. This results in a blurred field-line tracing of the magnetic surface, giving the surfaces in Fig. 2 radial widths of 2-8 mm. This dimension is comparable to the 8-mm difference in the amplitude of the ripple from inboard to outboard locations in the equatorial plane.

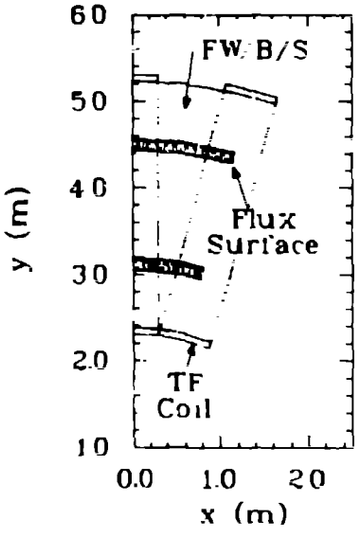

Fig. 2. The puncture plots (the intersection of a field line with the equatorial plane) for starting minor radii of 0.63, 0.67, 0.71, and 0.75 m and toroidal angle of $\pi/48$ displayed in one field period. The reversal surface occurs at $r_v \approx 0.64$ m.

The radial width of the flux surfaces is not a concern for an RFP unless this width becomes larger than the distance $\delta' = r_p - r_v$. As confinement is thought to occur primarily in this region, field lines which connect the central plasma directly to the plasma surface would short circuit the confinement process. The basic configuration is acceptable with respect to this constraint, since the surface width of 2-8 mm is much smaller than $\delta' \approx 70$ mm.

B. Three-Dimensional Divertor Designs

B.1. Bundle Divertor (BD). The BD offers strong maintenance advantages associated with a plug-in capability.[6] The physical layout and

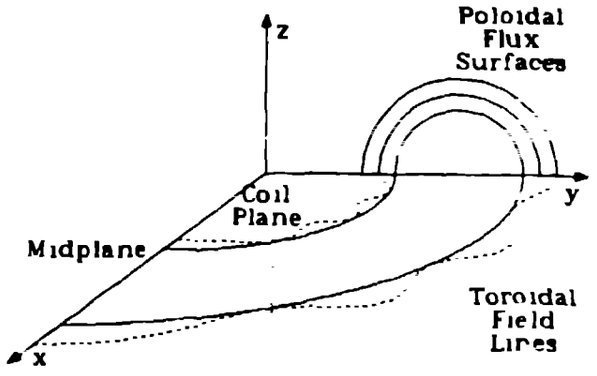

Fig. 3. Asymmetric toroidal-field ripple shown in the equatorial plane. Toroidally symmetric, nested-poloidal-flux surfaces connect inboard toroidal-field lines to outboard field lines.

parameters for the basic configuration with 24 BDs is shown in Fig. 4 and Table II. The edge plasma calculations reported in Ref. 6 indicated a BD connection length of ~35 m is needed, above which appreciable cross-field diffusion to the first-wall is expected to occur. A field line is traced for more than 300 m (> once around the torus) without entering any of the 24 divertor channels. The puncture plots associated with the field line tracing for the 24 BDs are also shown in Fig. 4. As a result of these inordinantly long connection lengths (> 1 km), most particle and associated energy loss would be transported to the first wall. Consequently, the toroidal-field bundle divertor is not considered feasible for the low-q RFP configuration.

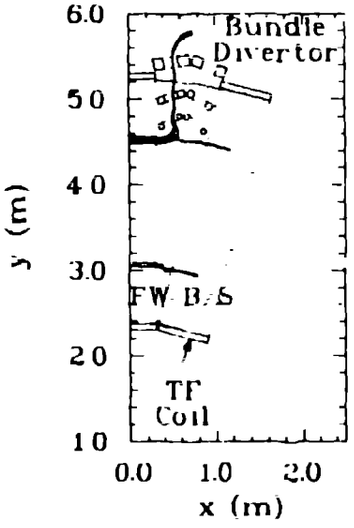

Fig. 4. The two-dimensional field-line tracings (solid lines) for 24 BDs for r = 0.69, 0.705, 0.715, 0.73, and 0.75 m on the outboard side and 0.71 and 0.75 m on the intoard side. Also shown is the puncture plot for the three-dimensional simulation of plasma and coils for r = 0.73 m.

B.2. Symmetric Divertor (SD). Interest in the SD principally rests with an inherently shorter connection length compared to the BD. The physical layout of a field period of the basic configuration with 4 SDs is shown in Fig. 5; design parameters are given in Table II. The TFCs have been thickened radially inward by 0.05 m, corresponding to the thickness of the defunct vacuum plenum needed for the limiter-based CRFPR design, in order to permit the unobstructed extraction of the divertor coils. The TFC cross-sectional area is preserved, however. The separatrix surface was symmetrized as best as possible to minimize the broadening of flux surfaces in the plasma at the expense of the symmetry of the divertor channel. Each divertor coil lies on a ray emanating from the major axis in order to symmetrize coil effects in toroidal angle. The centers of the divertor coils are shifted radially outward from the plasma center line in order to equalize the magnitude of the field perturbations produced by the divertor coils about the plasma as required by the 1/r dependence of the toroidal field. The field-line tracings for the two-dimensional simulation are also shown in Fig. 5, which also shows a puncture plot for a field line tracing started at r = 0.68 m and at a toroidal angle corresponding to half way between divertors. This puncture plot demonstrates good flux surfaces with radial width < 10 mm in the 70-mm-thick confinement region.

TABLE II
CRFPR DIVERTOR COIL DESIGN PARAMETERS

Toroidal-Field Bundle Divertor (BD)

Parameter(forward/middle/rear coil)	Value
Current (MA)	0.13/0.25/0.45
Major radius (m)	4.767/5.05/5.45
Height (m)	1.0/1.0/1.0
Width (m)	0.125/0.125/0.15
Current density (MA/m^2)	40/40/30
Angle (radians)	0.95/1.10/1.30

Toroidal-Field Poloidally Symmetric Divertor (SD)

Parameter(nulling/flanking coil)	Value
Current (MA)	-0.8/0.4
Major radius (m)	3.897/3.470
Minor radius (m)	1.088/0.970
Current density (MA/m^2)	50/40

The existence of a particle path into the divertor is also of interest. Shown in Fig. 5, is a combination of puncture plots for eighty field lines started at a toroidal location half way between SDs, each being equally spaced on a poloidal flux surface that passes through the point R = 3.07 m and terminated in the divertor coil plane. Such a calculation avoids the process whereby the asymmetry of the radial extent of the divertor channel in the divertor

coil plane takes a surface of small radial width upon entry into the divertor channel and greatly broadens the radial width of the surface upon exiting the divertor. This procedure nevertheless demonstrates that a path within the scrapeoff layer outside of the separatrix exists for particles to enter the divertor without first intersecting the first wall or reentering the plasma. The punctures are uniformly distributed poloidally for the first 0.2 m into the blanket, and are thereafter, distributed uniformly on the inboard side only. Future efforts will complete the SD symmetrization.

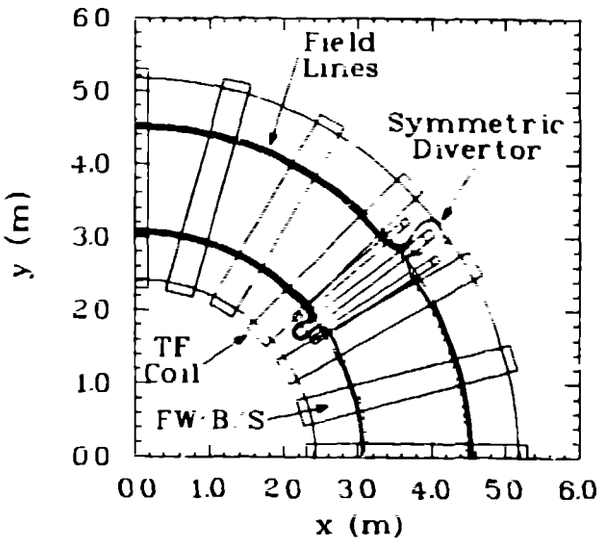

Fig. 5. The two-dimensional field-line tracings (solid lines) for 4 SDs for r = 0.69, 0.705, 0.715, 0.73, and 0.75 m. Also shown are the puncture plots for the three-dimensional simulation of plasma and coils r = 0.68 and 0.73 m.

The results of this calculation indicate a divertor connection length of 73.3 m and a connection length between divertor channel openings of 67.5 m. The two-dimensional calculations indicated the latter connection length to be 72.8 m for 4 SDs. The shorter connection length predicted by the full simulation results from the 1/r dependency of the toroidal field, the larger toroidal field on the inboard side more heavily weights the smaller major radius at that point. The results of the three-dimensional simulations of the SD indicate a small impact on the plasma and a reasonable connection length between divertor plates.

C. Design Parameters

An analytic scrapeoff model[13] has been applied to the SD. Table III summarizes results for a particle diffusivity $D = 1\ m^2/s$, a thermal diffusivity $\chi = 3D$, a radiation fraction, $f_{RAD} = 0.5$, a recycle coefficient, $R_{ie}^{*} = 0.98$, and a scrapeoff thickness, $x_{\ell} = 0.04$ m. The estimate of the incremental cost associated with divertors assumes that the cost of electricity (COE) scales inversely with net electric power. The blanket loss of 10.4% assumes no breeding between the outermost divertor coils, inclusively, and requires a tritium breeding ratio greater than 1.12.

TABLE III
DIVERTOR IMPACT ON CRFPR FUSION POWER CORE

Parameter	Value	
	2-D	3-D
Number of divertors	4	
Blanket loss (%)	10.4	
Ohmic power (MW)	47.7	
COE increase (%)	5.0	
First-wall area decrease (%)	5.36	
Divertor/first-wall area	0.65	
Divertor efficiency	0.93	0.94
Power to first wall(MW)	305.7	304.3
Power to divertor(MW)	266.1	267.5
First wall heat flux (MW/m^2)	2.87	2.86
Divertor heat flux (MW/m^2)	3.82	3.84
Typical edge plasma conditions		
• Edge-plasma temperature (eV)	143.4	147.7
• Wall-plasma temperature (eV)	50.	
• Edge-plasma density ($10^{20}/m^3$)	1.46	1.38

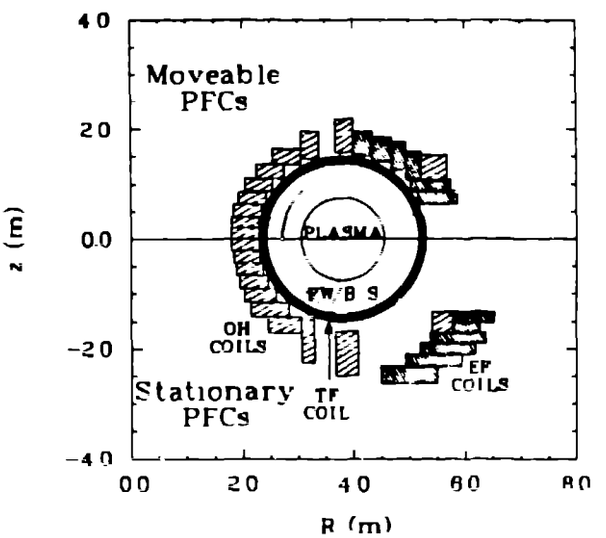

Fig. 6. The top half of the PFC set for the basic configuration and the bottom half of the PFC set for the easier divertor maintenance scheme. Also shown is the puncture plot (the field line intersections with the equatorial plane) for the three-dimensional simulation of plasma and coils.

The divertor maintenance can be accomplished in one of two ways. The outboard quadrants of the PFC set can be simultaneously raised and lowered to permit horizontal extraction. An ~0.7-m vertical lift is required for the PFC set, as shown in the upper half of Fig. 6. A second, less-complicated

maintenance scheme allows a PFC clearance that is sufficient to permit horizontal extraction. This latter design is shown in the lower half of Fig. 6, and would dissipate an additional 19.1 MW of Ohmic power in the PFC set. Both PFC designs provide access to the high performance coils and divertor channel surfaces, where frequent maintenance is expected.

IV. CONCLUSIONS

The three-dimensional simulation of both plasma and coils indicates that the broadening of flux surfaces because of toroidal-field ripple asymmetries is more important than the magnetic islands expected from the toroidal-field ripple. Flux surface broadening should be present in any toroidal device with TFCs and another toroidally symmetric field coil set (e. g., tokamaks).

The SD is clearly preferable to the BD on the basis of reduced connection length. The presence of an SD does not significantly perturb the flux surfaces in the outer region of the RFP plasma and, therefore, should not significantly affect confinement. The SD preserves the compactness of the fusion power core in a maintainable geometry. Preliminary analysis inidicate managable heat fluxes (~ 3 MW/m^2) on all surfaces for a modest cost penalty, $\sim 5\%$. The results of this study indicate a more detailed design is warrranted.

REFERENCES

1. R. L. HAGENSON, et al., "Compact Reversed-Field Pinch Reactors (CRFPR): Preliminary Engineering Considerations," Los Alamos National Laboratory report LA-10200-MS (August 1984).

2. R. L. HAGENSON, R. A. KRAKOWSKI, C. G. BATHKE, and R. L. MILLER, "The Reversed-Field Pinch: A Compact Approach to Fusion Power," Los Alamos National Laboratory document LA-UR-84-2410, Proc. 10th Int. Conf. on Plasma Physics and Controlled Nuclear Fusion Research, paper IAEA-CN44/H-II-5, London, 12-19 September, 1984.

3. F. WAGNER, M. KEILHACKER, and the ASDEX and NI Teams, "Importance of the Divertor Configuration for Attaining the H-Regime in ASDEX," J. Nucl. Mater. 121, 103 (1984).

4. S. M. KAYE, et al., "Attainment of High Confinement in Neutral Beam Heated Divertor Discharges in the PDX Tokamak," ibid., p. 115.

5. W. PFEIFFER, AND R. E. WALTZ, "Empirical Scaling Laws and Energy Confinement in Ohmically-Heated Tokamaks," Nucl. Fusion 19, 51 (1979).

6. C. G. BATHKE, R. L. MILLER, and R. A. KRAKOWSKI, "Magnetic Divertor Design For The Compact Reversed Field Pinch Reactor," Proc. 13th Sym. on Fus. Tech., Varese, Italy (September 24-28, 1984).

7. C. COPENHAVER, et al., "Fusion-Power-Core Design of a Compact Reversed-Field Pinch Reactor (CRFPR)," Proc. 6th Topical Meet. on the Technol. of Fusion Energy (March 3-7, 1985) (to be published in Fusion Technol, 1985).

8. J. F. PARMER, R. A. SUTTON, S. L. AGARWAL, and M. W. LIGGETT "Design of the MARS Magnet Set," Proc. 13th Sym. on Fus. Tech., Varese, Italy (September 24-28, 1984).

9. R. L. MILLER, et al., "The Modular Stellarator Reactor: A Fusion Power Plant," Los Alamos National Laboratory report LA-9737-MS (July 1983).

10. K. F. SCHOENBERG, R. F. GRIBBLE, and J. A. PHILLIPS, "Zero-Dimensional Simulations of Reversed-Field Pinch Experiments," Nucl. Fusion 22, 1433 (1982).

11. P. THULLEN and K. F. SCHOENBERG, Eds., "ZT-H Reversed Field Pinch Experiment Technical Proposal," Los Alamos National Laboratory document LA-UR-84-2602 (June 1984).

12. R. L. SPENCER, "Magnetic Islands and Stochastic Field Lines in the RFP," Proc. RFP Theory Workshop, Los Alamos, NM (April 29-May 2, 1980), Los Alamos National Laboratory report LA-8944-C, p. 129 (January 1982).

13. H. C. HOWE, "Physics Considerations for the FED Limiter," Oak Ridge National Laboratory report ORNL/TM-703 (July 1982).